

Pyrrolidinium Cation-based Ionic Liquids with Different Functional Groups: Butyl, Butyronitrile, Pentenyl, and Methyl Butyrate

Byeongjin Baek, Sangjun Lee, Cheolsoo Jung*

Department of Chemical Engineering, University of Seoul, 163 Shiripdae-gil, Dongdaemun-gu, Seoul 130-743, Korea

*E-mail: csjung@uos.ac.kr

Received: 22 August 2011 / Accepted: 7 November 2011 / Published: 1 December 2011

Four pyrrolidinium (PY)-based ILs were synthesized from TFSI ions and PY⁺ ions functionalized by butyl, butyronitrile, pentenyl, and methyl butyrate as an electrolyte for Li ion batteries. The ILs with a lower T_m had a much higher viscosity and lower conductivity because of the biased electron distribution in their quaternary ammonium cations. The potential windows of the ILs demonstrated stability above 5.0 V and all of the synthesized ILs showed evidence of forming a SEI layer on the graphite electrode. The peak currents for reduction on the graphite electrode and for oxidation on the LiCoO₂ electrode were 100 times stronger in PY(butyl)TFSI and PY(pentenyl)TFSI than in PY(butyronitrile)TFSI and PY(methyl butyrate)TFSI. This difference resulted from the electrolyte conductivity which is deeply related to the solvation strength between Li⁺ ions and the functional groups of the ILs.

Keywords: Ionic liquid, functional group, pyrrolidinium, Li ion batteries

1. INTRODUCTION

Recently, ionic liquids (ILs) have attracted much attention across many fields due to their favorable physicochemical properties such as thermal stability, high ionic conductivity, non-flammability, and negligible volatility [1, 2]. Previously reported ILs generally contained bulky and asymmetric organic cations such as ammonium [3, 4], phosphonium [5], imidazolium [6], and guanidinium [7] to maintain their liquid state at room temperature. Their counter anions are also important to maintain the liquid state and may include many types ranging from halide ions (Br⁻, Cl⁻) to composite anions such as [Ag(CN)₂]⁻, [BF₄]⁻, [PF₆]⁻, [AsF₆]⁻, [N(CF₃SO₂)₂]⁻, and [CF₃CONCF₃SO₂]⁻ [8]. In addition, ILs have been researched as substitute materials for organic solvents in various fields

including green solvents for organic synthesis or separation and electrochemical uses such as lithium ion batteries, electrochemical capacitors, dye-sensitized solar cells, and fuel cells [9-12]. These application possibilities are sure to be expanded further because ILs can be synthesized with special physicochemical and electrochemical properties similar to organic compounds. Ether-functionalized ILs are of particular interest as they can achieve superior electrochemical stability and high ionic conductivity. There have been many reports of ether-functionalized cations such as cyclic quaternary ammonium [3, 4], phosphonium [5], imidazolium [6], and guanidinium [7]. Nitrile-functionalized ILs are also interesting as they allow good cycling performances due to the formation of a good passivation layer during the cycling process, despite the fact that they have lower ionic conductivities and higher viscosities than ILs without nitrile substitution [13, 14].

The pyrrolidinium (PY) cation is a quaternary ammonium and has many advantages as the cation part of ILs because of its structure and various properties. In this study, PY^+ ions were functionalized by butyl, butyronitrile, pentenyl, and methyl butyrate groups. In addition, the physicochemical and electrochemical properties of their ILs with TFSI as the counter ion were investigated to investigate the possibility as an electrolyte for Li ion batteries.

2. EXPERIMENTAL

2.1 Materials

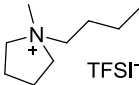
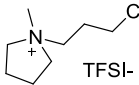
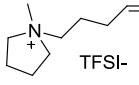
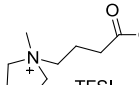
N-methylpyrrolidine (PY, Aldrich, > 97%), 1-bromobutane (Tokyo Kasei Co. > 98%), 4-bromobutyronitrile (Aldrich, > 97%), 5-bromo-1-pentene (Tokyo Kasei Co., > 95%), methyl-4-bromobutyrate (Tokyo Kasei Co., > 98%), and magnesium sulfate (Junsei Co.) were pretreated overnight using 4A molecular sieve (Aldrich). All solvents, ethyl acetate (SamChun Chem., > 99.9%), dimethylether (Junsei > 99.5%), and anhydrous dichloromethane (Aldrich), were dried and purified using general procedures [15]. Battery grade lithium bis(trifluoromethylsulfonyl)imide (LiTFSI) was supplied by Techno Semichem Co., Ltd.

2.2 Synthesis and characterization

The synthesis of the ILs used in this study was based on a quaternization reaction of *N*-methylpyrrolidine (PY) with four kinds of linear bromo-compounds with similar chain lengths: 1-bromobutane, 4-bromobutyronitrile, 5-bromo-1-pentene, and methyl-4-bromobutyrate. The precursors, PYBr, of the designed ILs were prepared by reacting *N*-methylpyrrolidine (PY) and a linear bromo-compound in ethyl acetate at 40°C for 36 hrs under reflux conditions [16, 17]. After cooling, the precursors were washed with dimethylether until white salts formed. Equimolar amounts of the purified precursor (PYBr) and LiTFSI were dissolved in deionized (DI) water and stirred for 24 hrs at room temperature to facilitate the exchange reaction of Br^- ions with TFSI. The upper phase of the reacting solution was removed and the remaining phase was washed 5 times with fresh hot DI water to remove any remaining LiBr. This viscous liquid was also treated with activated carbon and alumina

with ethyl acetate to remove impurities. The solvent was removed by rotary evaporation and the final products (PY(pentenyl)TFSI, PY(butyl)TFSI, PY(butyronitrile)TFSI, and PY(methyl butyrate)TFSI) were dried in a vacuum oven at 80°C for 24 hrs and then at 100°C for 5 hrs. The resulting colorless liquids were stored in a glove box (< 10 ppm H₂O). The chemical structures of the synthesized ILs are shown in Table 1.

Table 1. Chemical structures of the four synthesized ionic liquids.

	PY(butyl) TFSI	PY(butyroCN) TFSI	PY(pentenyl) TFSI	PY(methyl butyrate)TFSI
Chemical Structure				

- TFSI⁻ is the bis(trifluoromethylsulfonyl)imide anion

The water contents of the ILs were measured by Karl-Fischer titration (< 0.05 wt.%). The structures of the synthesized ILs were analyzed by FTIR (Perkin Elmer Co.), and H¹ and C¹³ NMR (Bruker, Avance 400).

PY(butane)TFSI – PY(butyl)Br (CDCl₃): ¹H NMR δ 3.48-3.27 (m 6H), 2.98 (s 3H), 2.08 (br s 4H), 1.70-1.64 (m 2H), 1.35-1.29 (m 2H), 0.96-0.92 (m 2H); ¹³C NMR δ 65.62-65.06, 49.75-49.67, 32.87, 27.11, 23.27, 21.49, 15.68 / PY(butane)TFSI (d₆-DMSO): ¹H NMR δ 3.49-3.46 (br m 4H), 3.35-3.30 (br m 2H), 3.00 (s, 3H), 2.13 (br s 4H), 1.75-1.68 (m 2H), 1.38-1.33 (m, 2H), 0.98-0.93 (m 2H); ¹³C NMR δ 124.26-114.67, 63.42-63.10, 47.44-47.37, 24.82, 20.89, 19.07, 12.91

[PY(butyronitrile)TFSI] – PY(butyronitrile)Br (CDCl₃): ¹H NMR δ 4.07-4.03 (m 2H), 3.97-3.91 (br m 2H), 3.76-3.74 (br m 2H), 3.31 (s 3H), 2.80-2.76 (t 2H), 2.42 (b 2H), 2.35-2.26 (br m 4H); ¹³C NMR δ 118.41, 65.06, 62.45, 48.99, 21.73, 20.78, 14.72 / PY(butyronitrile)TFSI (d₆-DMSO): ¹H NMR δ 3.53-3.43 (br m 4H), 3.39-3.35 (br m 2H), 3.00 (s 3H), 2.64-2.60 (t, 2H), 2.09-2.039 (br m, 6H); ¹³C NMR δ 124.26-114.66, 63.66, 61.43, 47.61, 47.58, 21.01, 19.42, 13.77

[PY(pentene)TFSI] - PY(pentenyl)Br (d₆-DMSO): ¹H NMR δ 5.85-5.78 (m 1H), 5.12-5.01 (m 2H), 3.54-3.45 (m br 4H), 3.37-3.33 (m, 2H), 3.02 (s 3H), 2.08-2.04 (m br, 6H), 1.85-1.77 (m 2H); ¹³C NMR δ 136.95, 115.88, 63.42-63.36, 62.51, 47.54-47.47, 29.84, 22.15, 21.03 / PY(pentene)TFSI: ¹H NMR δ 5.89-5.76 (m 1H), 5.13-5.03 (m 2H), 3.52-3.39 (m br, 4H), 3.31-3.27 (m 2H), 2.99 (s, 3H), 2.09-2.06 (t, 6H), 1.86-1.77 (m 2H); ¹³C NMR δ: 136.85, 124.26-114.66, 115.92, 63.48, 63.48-63.43, 62.67, 47.55-47.47, 29.83, 22.09, 21.03.

[PY(butyrate)TFSI] - PY(butyrate)Br (d₆-DMSO): ¹H NMR δ 3.63 (s 3H), 3.52 (b, 2H), 3.43 (b, 2H), 3.35 (b, 2H), 3.01 (s, 3H), 2.49-2.41 (t, 2H), 2.09 (br s, 4H), 2.01-1.93 (m, 2H); ¹³C NMR δ 172.29, 63.47, 61.99, 51.53, 47.50, 29.99, 21.05, 18.68 / PY(butyrate)TFSI: ¹H NMR δ 3.63-3.62 (d,

23H), 3.52-3.38 (m br 4H), 3.33-3.28 (m 2H), 2.99 (s, 3H), 2.44-2.41 (t, 2H), 2.09 (s br, 4H), 1.999-1.95 (m 2H); ^{13}C NMR δ 172.28, 124.25-114.65, 63.53-63.47, 62.05, 51.49, 47.52-47.45, 29.94, 21.03, 18.65

2.3 Physical properties

The viscosity (η) was measured by a Brookfield DV-II with an ultra adapter. The ionic conductivity (σ) was measured on Sus/IL/Sus hermetically sealed cells using an AC impedance analyzer (Zahner Elektrik). The thermal properties of the ILs were measured by differential scanning calorimetry (DSC 8000, Perkin Elmer Co.) and thermogravimetric analysis (Pyris 1 TGA, Perkin Elmer Co.) under a N_2 flux. The heating rates in the DSC and TGA measurements were 10 and 20°C min^{-1} , respectively. FT-IR spectra were obtained from 400 to 4,000 cm^{-1} on a PXI (Perkin Elmer Co.) with a resolution of 8 cm^{-1} .

2.4 Electrochemical properties

The electrochemical stabilities of the synthesized ILs were evaluated by linear sweep voltammetry (LSV) at a scan rate of 5 mV s^{-1} at 20°C in a glove box (< 10 ppm H_2O). A Pt electrode ($d = 0.2$ cm) was used as the working electrode and lithium metal was used as the counter and reference electrodes. Before the LSV measurements, the Pt electrode was polished with a diamond slurry (15 μm , BASI). In this study, the anodic process was scanned from 3.0 to 6.0 V separately from the cathodic process, which was scanned from 3.0 to 0 V (Li/Li^+). The electrochemical behaviors of the ILs on a graphite or LiCoO_2 electrode were acquired at 20°C by cyclic voltammetry (CV) at a scan rate of 0.05 mV s^{-1} using a scanning electrochemical microscope (CHI900B) in a glove box. The electrodes, graphite, and LiCoO_2 were supplied as mass production grade from Enerland Co. and the sizes of the electrodes resulted in a reaction area with a radius of 3.22 mm. Each electrolyte was prepared by mixing 0.75 mol kg^{-1} LiTFSI in each synthesized IL for the LSV and CV measurements.

3. RESULTS AND DISCUSSION

3.1 Solubility of LiTFSI in the Pyrrolidinium precursor

The solubility of Li salt in the pyrrolidinium precursor is a very important factor to complete the electrolyte using the ILs of the pyrrolidinium series. In this research, the pyrrolidinium precursors were synthesized by a quaternization reaction of *N*-methylpyrrolidine (PY) and the four linear bromo-compounds with similar chain lengths: 1-bromobutane, 4-bromobutyronitrile, 5-bromo-1-pentene, and methyl-4-bromobutyrate. The precursor and LiTFSI were mixed at 80°C for 24 hr and then cooled to room temperature. Up to 1.5 mol/kg and 1.75 mol/kg of LiTFSI was dissolved completely in PY(butyl)Br and PY(pentenyl)Br, respectively. On the other hand, PY(butyronitrile)Br and PY(methyl butyrate)Br could sufficiently dissolve over 1.75 mol kg^{-1} LiTFSI, indicating that TFSI $^-$ ions can

solvate with PY⁺ ions well when the butyronitrile and methyl butyrate groups are substituted with PY⁺ ions. As a result, the solubility of LiTFSI to PYBr can be qualitatively ranked as follows: PY(methyl butyrate)Br \approx PY(butyronitrile)Br > PY(pentenyl)Br > PY(butyl)Br. Therefore, all ILs used in this study were fabricated using 1.25 mol kg⁻¹ LiTFSI in the purified precursor (PYBr).

3.2 Physicochemical properties

In this research, the ILs were synthesized from TFSI ions and PY⁺ ions functionalized by butyl, butyronitrile, pentenyl, and methyl butyrate.

Table 2. Physicochemical properties of the four synthesized ionic liquids.

Ionic Liquids	M.W g mol ⁻¹	T _c / °C	T _m / °C	T _d ^a / °C	η^b / mPa s	σ^c / mS cm ⁻¹
PY(butyl)TFSI	422.4	-57.5	-19.8	437	91.8	1.69
PY(butyronitrile)TFSI	433.4	nd ^d	-67.2	442	399.0	0.46
PY(pentenyl)TFSI	434.4	-71.9	-3.7	405	90.6	1.15
PY(methylbutyrate)TFSI	466.4	nd ^d	-72.4	387	211.2	0.79

^a 5 % weight loss of Ionic liquid calculated on TGA

^b Viscosity at 20 °C

^c Ionic conductivity at 20 °C

^d nd = not detected

As summarized in the physical property parameters shown in Table 2, all of the ILs have melting points below 0°C and PY(butyronitrile)TFSI and PY(methyl butyrate)TFSI maintain their liquid state to *ca.* -70°C. Quaternary ammonium ILs are reported to have relatively low melting points because of the structural asymmetry of their cations [18, 19, 20]. This asymmetric structure can prevent them from ideal packing in solid-state lattices allowing maintaining the liquid state even at a lower temperature. The much lower observed melting points of PY(butyronitrile)TFSI and PY(methyl butyrate)TFSI than those of reported ILs with PY⁺ ions, however, could not be explained simply by the asymmetrical structure because these four PY functional groups have almost the same chain length. The biased electron distribution can be a reasonable explanation for these much lower melting points. Both butyronitrile and methyl butyrate groups are more powerful electron-withdrawing groups than butyl and pentenyl groups. Therefore, these functional groups can change the electron distribution in the whole molecular system of the ILs. Usually, organic compounds with a polar group have a high melting point because they experience stronger interactions among themselves. However, these biased electron distributions of PY(butyronitrile) and PY(methyl butyrate) cations make it difficult to form the crystalline structure in sterically bulky PY⁺ ions, as compared to PY(butyl) and PY(pentenyl) cations. Typically, crystalline temperatures (T_c) of -57°C and -72°C are observed for PY(butyl)TFSI and PY(pentenyl)TFSI in DSC measurements, but crystalline temperatures were not detected down to -90°C for PY(butyronitrile)TFSI and PY(methyl butyrate)TFSI. This means that the crystallization of

PY(butyronitrile)TFSI and PY(methyl butyrate)TFSI is disturbed by the biased electron distributions in their asymmetric chemical structures.

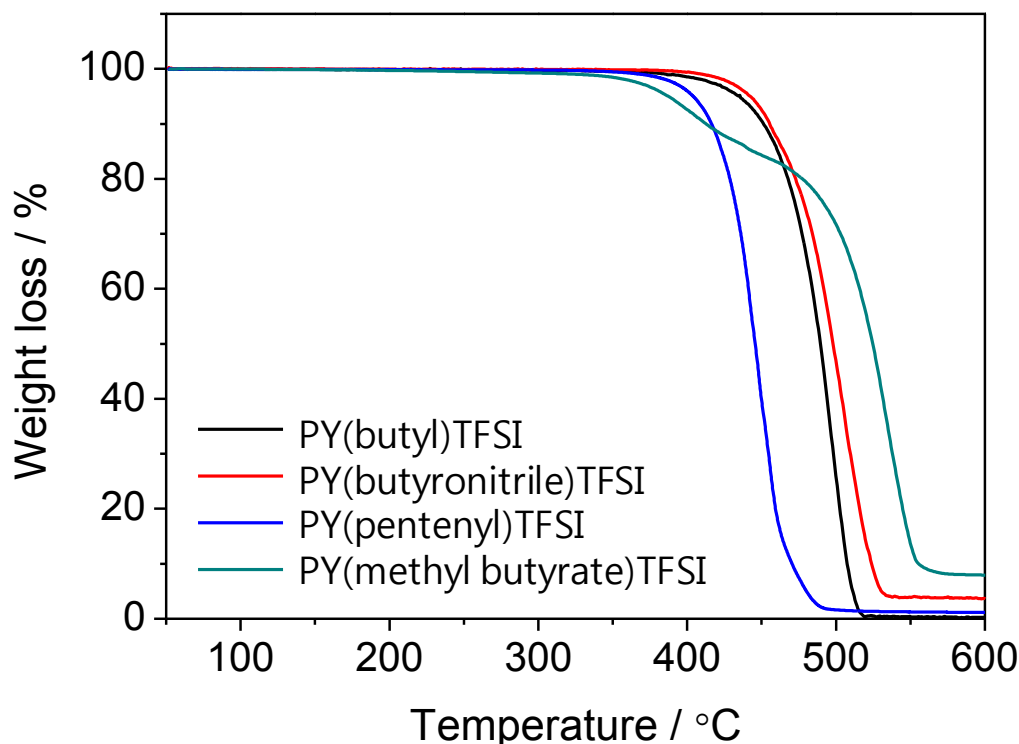


Figure 1. TGA thermograms of the synthesized ionic liquids between 50 and 600°C at a scan rate of 20°C min⁻¹.

The thermal stabilities of the ILs were measured by TGA in the range of 50 to 600°C. As shown in Fig. 1, the ILs except for PY(methyl butyrate)TFSI are thermally stable to 400°C. The point of 5 wt.% loss was considered as the decomposition temperature (T_d) of the ILs. As listed in Table 2, the T_d is in the order of PY(butyronitrile)TFSI (442°C) \approx PY(butyl)TFSI (437°C) > PY(pentenyl)TFSI (405°C) > PY(methyl butyrate)TFSI (387°C). That is, pentenyl and methyl butyrate groups decompose more easily than butyl and butyronitrile groups at high temperature. In addition, PY(pentenyl)TFSI, PY(butyronitrile)TFSI, and PY(butyl)TFSI show one-step decomposition behavior, whereas PY(methyl butyrate)TFSI decomposes in two steps. These results represent typical thermal behavior of these functional groups, as it has been reported that methoxyethyl-substituted ILs are less thermally stable than hydrocarbon alkyl-substituted ILs [21] and the thermal stability decreases when introducing a methyl acetate group to imidazolium, pyrrolidinium, morpholinium, and piperidinium cations [22].

The viscosities of the synthesized ILs were measured at 20°C and are listed at Table 2. The data shows there is a close connection between their melting points and viscosities, different than the thermal stability at high temperature. The ILs with a lower T_m have higher viscosities of 399 and 211.2 mPa s for PY(butyronitrile)TFSI and PY(methyl butyrate)TFSI, respectively. On the contrary, the ILs with a higher T_m , PY(butyl)TFSI and PY(pentenyl)TFSI, have the lowest viscosities of 91.8 and 90.6 mPa s, respectively. These physical properties can also be explained by the biased electron distribution

of PY⁺ ions functionalized by butyl, pentenyl, methyl butyrate, and butyronitrile. Butyl and pentenyl groups can easily act as an electron donor to PY⁺ ions, weakening the electrostatic interactions with TFSI ions and leading to a decrease of viscosity. Since butyronitrile and methyl butyrate groups are electron withdrawing groups, on the contrary, the cationic property of the pyrrolidinium ring increases with PY(butyronitrile)TFSI and PY(methyl butyrate)TFSI. Thus, the increased electrostatic interaction between PY⁺ ions and TFSI ions makes these ILs more viscous. The difference of the electronic distributions of the PY⁺ ions can be confirmed from the H¹ NMR analysis. In H¹ NMR spectroscopy, the value of the chemical shift depends on electronic effects of the molecular structure, especially the polarity of adjacent groups. Generally, nuclei tend to be deshielded by groups which withdraw electron density and deshielded nuclei resonate at higher δ values, whereas shielded nuclei resonate at lower δ values. The chemical shift of the proton attached to the 1st carbons of pyrrolidinium amine was assigned to a higher δ value in PY(butyronitrile)TFSI and PY(methyl butyrate)TFSI than in PY(butyl)TFSI and PY(pentenyl)TFSI. This means that the electron density of PY⁺ ions in PY(butyronitrile)TFSI and PY(methyl butyrate)TFSI is not as dense as that in PY(butyl)TFSI and PY(pentenyl)TFSI.

Generally, the viscosity of a fluid such as ILs has a temperature dependence which follows the Vogel-Fulcher-Tammann (VFT) equation (1) [2]:

$$\eta = \eta_0 \exp\left(\frac{B}{T - T_0}\right) \quad (1)$$

where η_0 (mPa s) is a pre-exponential factor, B (K) is the pseudo-activation for a viscous liquid, and T_0 (K) is the ideal glass transition temperature. The viscosities of the ILs synthesized in this research fit the VFT equation well, as shown in Fig. 2.

Table 3. VFT equation parameters used to calculate the viscosities of the ILs.

	$\eta_0 / 10^{-1} \text{ mPa s}$	$B / 10^2 \text{ K}$	$T_0 / 10^2 \text{ K}$	R^2
PY(butyl)TFSI	$0.88 \pm 2.0 \%$	$10.66 \pm 0.7 \%$	$1.40 \pm 0.4 \%$	0.999
PY(butyronitrile)TFSI	$0.06 \pm 0.1 \%$	$12.74 \pm 0.1 \%$	$1.48 \pm 0.1 \%$	0.999
PY(pentenyl)TFSI	$1.85 \pm 0.3 \%$	$8.05 \pm 0.1 \%$	$1.63 \pm 0.1 \%$	0.999
PY(methylbutyrate)TFSI	$0.17 \pm 0.3 \%$	$8.45 \pm 0.1 \%$	$1.74 \pm 0.1 \%$	0.999
-The percentage standard error for the parameters and R^2 is the VFT fitting parameter error.				

The R^2 values in Table 3 show that the four ILs follow the VTF equation closely in range of 20-70°C. According to the VTF parameters, the higher viscous ILs have lower η_0 values, but the other parameters (B and T_0) do not show a distinct relationship with viscosity.

The temperature dependence of the conductivity was also analyzed using the Arrhenius equation (2):

$$\sigma = \sigma_0 \exp\left(\frac{E_a}{RT}\right) \quad (2)$$

where σ_0 is a pre-exponential factor, E_a is the activation energy, and R is the ideal gas constant.

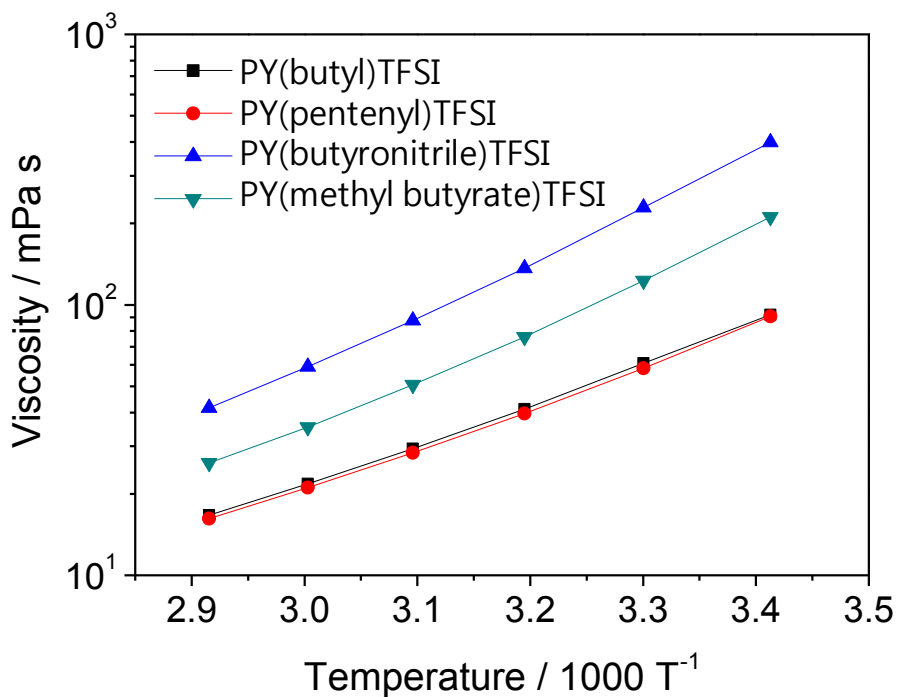


Figure 2. VTF plots of the viscosity of the synthesized ionic liquids with different functional groups of the pyrrolidinium cation.

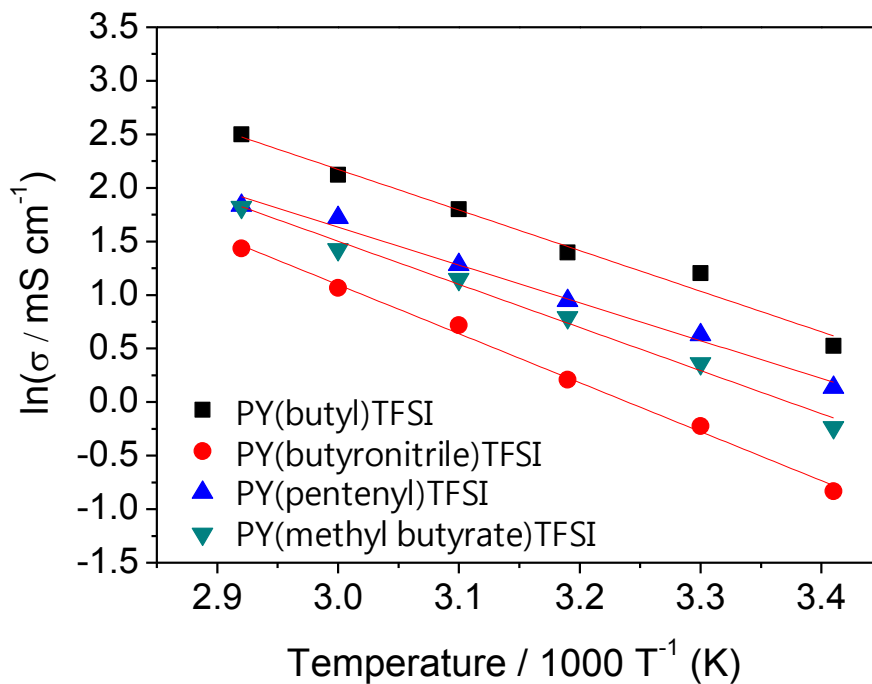


Figure 3. Arrhenius plots of the conductivity of the synthesized ionic liquids with different functional groups of the pyrrolidinium cation.

The conductivity data is plotted in Fig. 3 and the best fit parameters are listed in Table 4. The R^2 values show that the conductivity of the ILs fits the Arrhenius equation well. PY(butyronitrile)TFSI has a much higher σ_0 value than the other ILs. This implies that there is a distinct relationship between the electron withdrawing and donating properties.

Among these ILs, the butyronitrile group has the greatest electron withdrawing ability followed by the methyl butyrate group. The π -conjugated bond in the pentenyl functional group results in weak electron donating properties to the nitrogen of the PY^+ ions. Judging from the fitting parameters listed in Table 4, the ILs with a stronger electron withdrawing ability show higher E_a and σ_0 values. Inversely, the ILs with a higher electron donating ability have lower E_a and σ_0 values.

Table 4. Parameters of the Arrhenius conductivity equation.

	$\sigma_0 / 10^5 \text{ mS cm}^{-1}$	$E_a / \text{kJ mol}^{-1}$	R^2
PY(butyl)TFSI	6.81	31.21	0.984
PY(pentenyl)TFSI	1.81	29.03	0.989
PY(methylbutyrate)TFSI	6.99	33.14	0.992
PY(butyronitrile)TFSI	23.67	37.65	0.997

It is necessary to design ILs with a lower viscosity because the viscosity of the electrolyte is directly correlated to the transport of Li^+ ions in Li ion batteries. In general, the conductivity of the liquid electrolyte is inversely correlated with its viscosity via the Stokes-Einstein and Nernst-Einstein relationships [1, 24]:

$$\sigma = \frac{cz^2F^2}{6\pi r N_a \eta} \quad (3)$$

where N_a is the Avogadro number, c is the molar concentration, z is the ion valance, F is the Faraday constant, and r is the radius of the spherical ion. Because the electrolyte with high viscosity hinders the mobility of ions in the bulk electrolyte, highly viscous ILs have lower ionic conductivities. For PY(butyronitrile)TFSI, PY(methyl butyrate)TFSI, and PY(pentenyl)TFSI, their conductivity is inversely proportion to viscosity, which is directly connected with the intensity of their biased electron distribution. That is, the stronger interactions with Li^+ ions results in a decreased conductivity, as in the case of PY(butyronitrile)TFSI and PY(methyl butyrate)TFSI. Even though the viscosity of PY(butyl)TFSI is nearly the same as that of PY(pentenyl)TFSI, the conductivity of PY(butyl)TFSI is much higher than that of PY(pentenyl)TFSI, as shown in Table 2.

The results indicate that Li^+ ions interact more strongly with the ethylene group moiety of the pentenyl group than the butyl group. However, the difference of the conductivities between PY(butyl)TFSI and PY(pentenyl)TFSI does not produce a large gap of the current on the graphite or the LiCoO_2 substrate in CV experiments.

3.4 Electrochemical stability and battery performance

The electrochemical potential windows of the four ILs were investigated by LSV measurements on a Pt electrode and were compared based on a cut-off current of 0.1 mA cm^{-2} . As shown in Table 5, the potential window order starting with the widest is PY(butyronitrile)TFSI > PY(methyl butyrate)TFSI \approx PY(butyl)TFSI > PY(pentenyl)TFSI. These differences are induced mainly by the anodic instability than cathodic decomposition, as shown in Fig. 4.

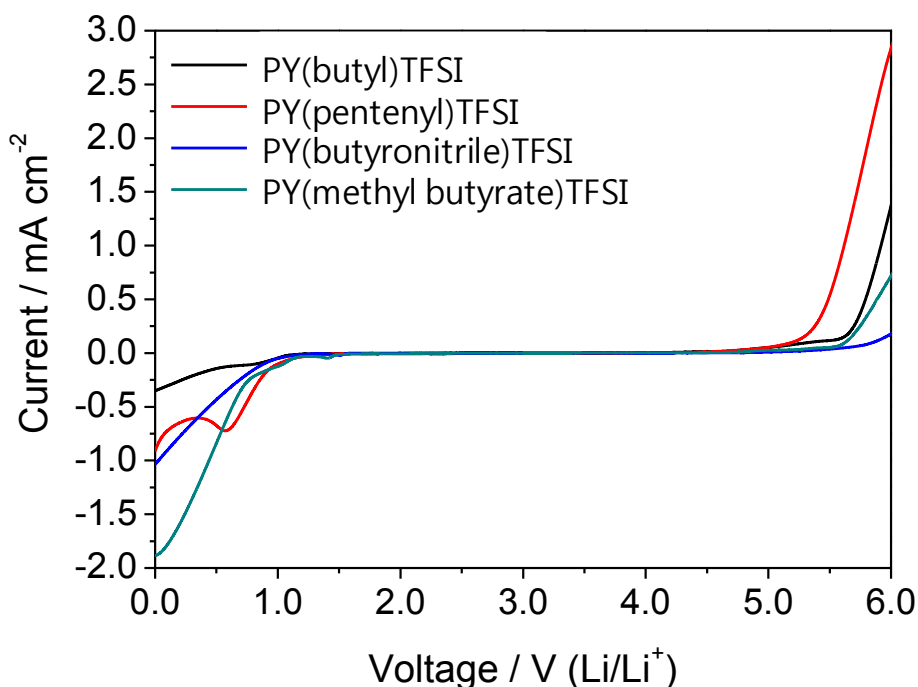


Figure 4. Linear sweep voltammograms for pure ionic liquids on a Pt electrode at a scan rate of 5 mV s^{-1} .

Table 5. Electrochemical windows of the synthesized ILs (vs. Li/Li^+).

Ionic Liquids	Cathodic Limit / V	Anodic Limit / V	Potential Window / V
PY(butyl)TFSI	0.83	5.34	4.51
PY(butyronitrile)TFSI	0.89	5.86	4.97
PY(pentenyl)TFSI	1.00	5.19	4.19
PY(methylbutyrate)TFSI	1.04	5.63	4.58
- Cut-off current density: 0.1 mA cm^{-2}			

In general, the anodic limits of ILs are determined by the oxidation of the anion [27], implying a dependence on the type of anion. Appetecchi *et al.* reported that anodic decomposition is due to the

oxidation of the TFSI⁻ ions and is moderately affected by the nature of the cation [24]. However, the ILs investigated in this study show different behaviors than previous studies. The four ILs have the same TFSI⁻ ion and the order of their anodic limits is PY(butyronitrile)TFSI (5.86 V) > PY(methyl butyrate)TFSI (5.63 V) > PY(butyl)TFSI (5.34 V) > PY(pentenyl)TFSI (5.19 V). These results mean that the ILs with high anodic stability can also be obtained by proper cation design. Generally, in organic chemistry, the allyl group is unstable due to its oxidizable π -bonding structure while cyanide and ester functional groups are more stable in the oxidizable region. These chemical properties can be applied to directly improve the electrochemical behavior of the ILs.

Meanwhile, the reduction behaviors of the ILs showed very unique properties with their structures, as shown in Fig. 4. PY(butyl)TFSI has a weak peak around 0.75 V and more stability than other structures, especially compared with PY(butyronitrile)TFSI, which decomposed increasingly without any special peak in the cathodic process. PY(pentenyl)TFSI also demonstrated cathodic decomposition as a stronger peak around 0.45 V than PY(butyl)TFSI. PY(methyl butyrate)TFSI also has a weak reduction peak at 1.4 V but the decomposition current increases gradually in the cathodic process, which is the same as PY(butyronitrile)TFSI.

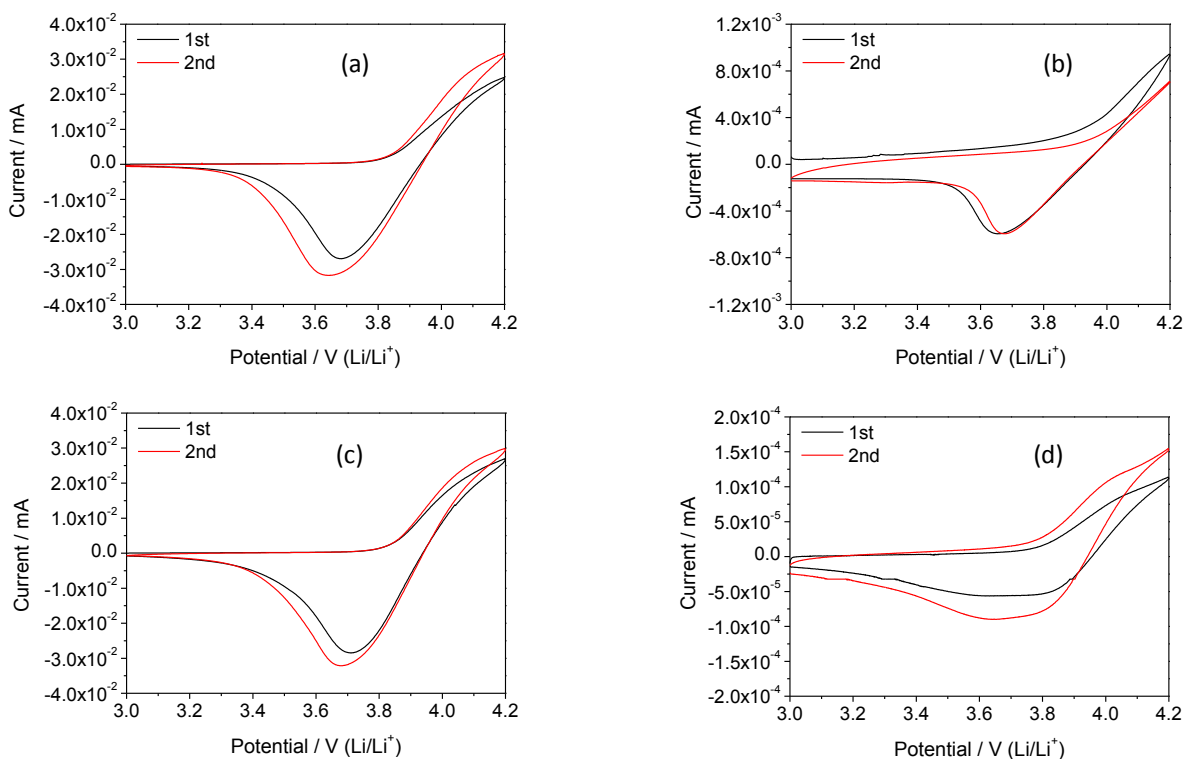


Figure 5. Cyclic voltammograms of four ionic liquids with 0.75 mol kg^{-1} LiTFSI on a LiCoO_2 electrode with a radius of 3.22 mm and a scan rate of 0.05 mV s^{-1} at 20°C : (a) PY(butyl)TFSI, (b) PY(butyronitrile)TFSI, (c) PY(pentenyl)TFSI, and (d) PY(methyl butyrate)TFSI.

Water contamination is often discussed as a possible cause of the cathodic decomposition observed around 1.0 V (vs. Li/Li⁺). Randström's group reported that this reduction peak does not

appear when the water content in the IL is below 1.0 ppm [26]. In this research, the water content was controlled at slightly less than 0.05 wt.% (500 ppm) in all of the synthesized ILs. If the cathodic currents were induced by water contamination, the behavior of the cathodic decomposition should be similar in all of the cases. From the results, it can be concluded that the cathodic and anodic decompositions of PY(functional group)TFSI are dependent on the structure of the functional group and the oxidation potentials of the synthesized ILs are in the sufficient potential range for use as the electrolyte for Li ion batteries.

In order to assess the feasibility for use as an electrolyte for Li ion batteries, cyclic voltammograms (CV) for each IL with LiTFSI (0.75 mol kg^{-1}) were obtained on LiCoO_2 (Fig. 5) and graphite (Fig. 6) electrodes, separately. As shown in the figures, all of the ILs have a decomposition peak around 1.0 V on the graphite electrode at the 1st cycle, which disappeared starting at the 2nd cycle, which is commonly regarded to be due to a typical solid electrolyte interface (SEI) layer formed on the graphite electrode. However, the peak currents at the reduction on the graphite electrode were 100 times stronger in PY(butyl)TFSI and PY(pentenyl)TFSI than in PY(butyronitrile)TFSI and PY(methyl butyrate)TFSI. Meanwhile, similar behaviors of the peak currents were observed on the LiCoO_2 electrode without the presence of a decomposition peak.

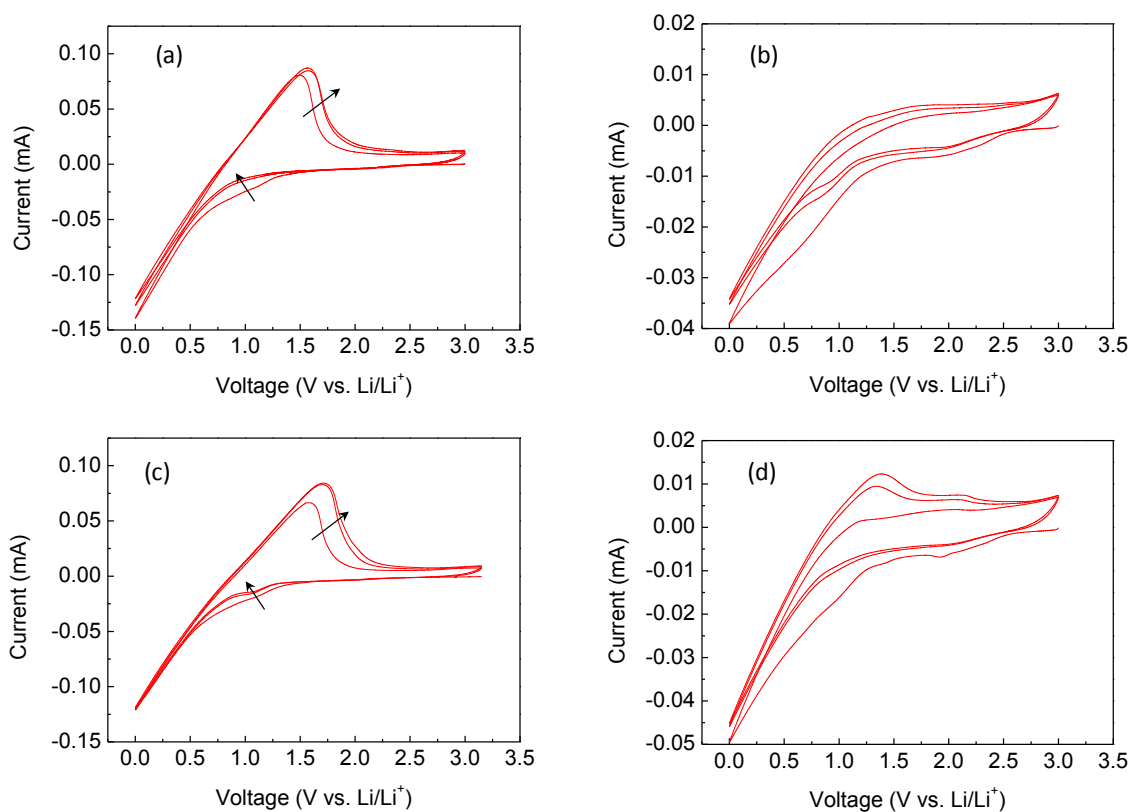


Figure 6. Cyclic voltammograms of four ionic liquids with 0.75 mol kg^{-1} LiTFSI on a graphite electrode with a radius of 3.22 mm radius and a scan rate of 0.05 mV s^{-1} at 20°C : (a) PY(butyl)TFSI, (b) PY(butyronitrile)TFSI, (c) PY(pentenyl)TFSI, and (d) PY(methyl butyrate)TFSI.

Therefore, it is clear that the difference of the currents results from the different electrolyte conductivities which are deeply related to the solvation strength between Li^+ ions and the functional groups of the ILs.

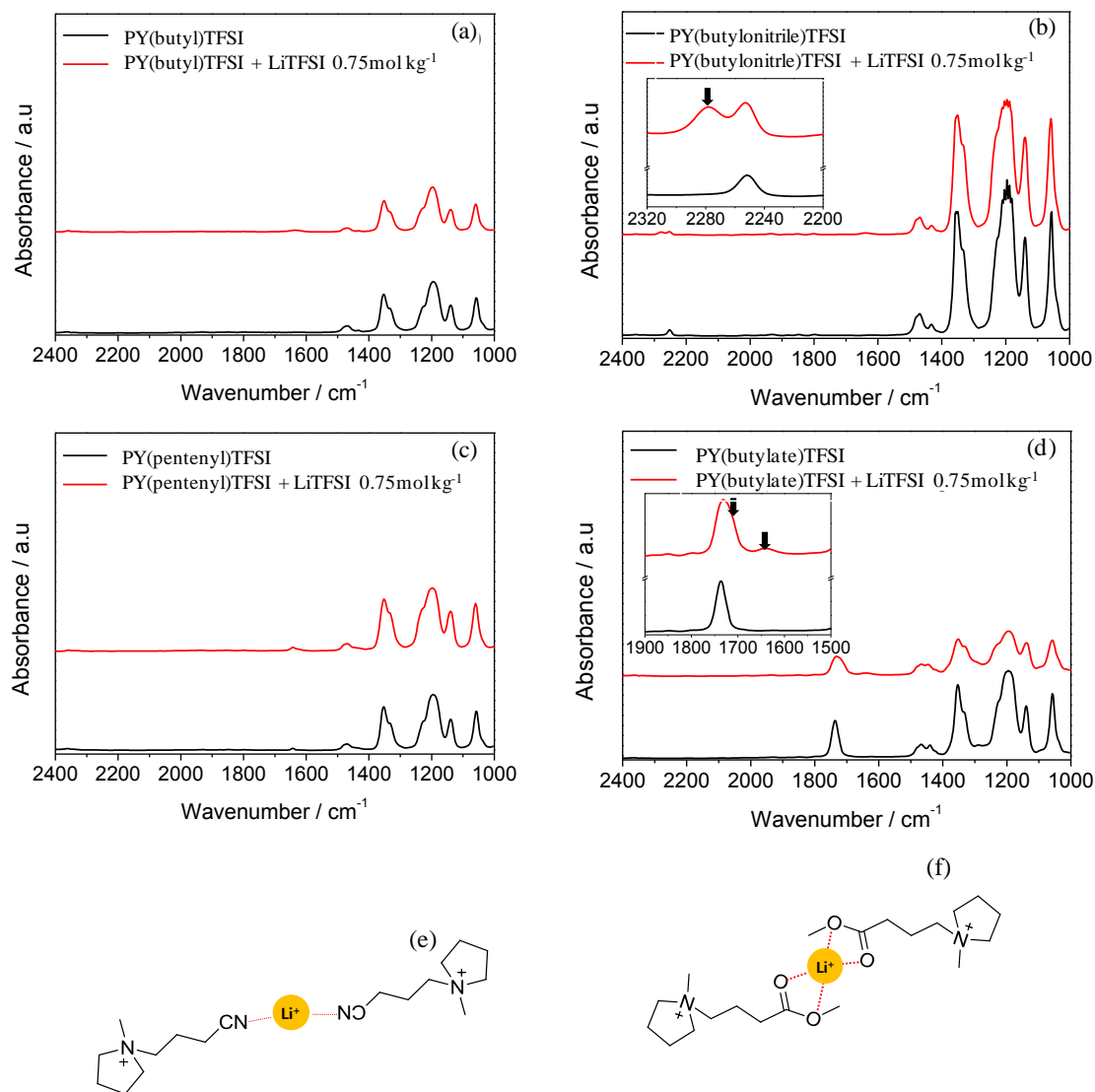


Figure 7. FT-IR absorbance spectra of ionic liquids according to the existence of LiTFSI : (a) PY(butyl)TFSI, (b) PY(butyronitrile)TFSI, (c) PY(pentenyl)TFSI, (d) PY(methyl butyrate)TFSI, and solvation scheme of (e) cyanide and (f) ester groups.

To verify this hypothesis, the FT-IR absorbance was evaluated for the synthesized ILs depending on LiTFSI addition. New peaks should be observable in the mixture of PY(functional group)TFSI and LiTFSI if there are interactions between the functional groups of the ILs and Li^+ ions [28]. As shown in Fig. 7, new peaks appear at $2,280 \text{ cm}^{-1}$ in PY(butyronitrile)TFSI (b) and at $1,650 \text{ cm}^{-1}$ and $1,720 \text{ cm}^{-1}$ in PY(methyl butyrate)TFSI (d) by adding TFSI ions. On the other hand, PY(butyl)TFSI (a) and PY(pentenyl)TFSI (c) did not show a significant difference before and after LiTFSI addition. These results indicate that the strong interaction between the polar functional groups

(cyanide and ester) and Li^+ ions forms an ionic cluster, which can obstruct the transport of Li^+ ions freely in the ILs, as illustrated in the schematic diagram in Fig. 7(e) and (f).

4. CONCLUSIONS

Four kinds of pyrrolidinium (PY)-based ILs were synthesized from TFSI ions and PY^+ ions functionalized by butyl, butyronitrile, pentenyl butyrate, and methyl butyrate. PY(butyl)TFSI and PY(pentenyl)TFSI had melting points (T_m) of -19.8°C and -3.7°C , respectively, and crystallization temperatures around -60°C . However, the melting points of PY(butyronitrile)TFSI and PY(methyl butyrate)TFSI were shifted to around -70°C . The ILs with a lower T_m had much higher viscosities and lower conductivities because of the biased electron distributions in their quaternary ammonium cations. On the other hand, the relationship of their conductivity and viscosity showed a typical trend following the Stokes-Einstein and Nernst-Einstein equations except for PY(butyl)TFSI, whose viscosity was nearly the same while its conductivity was much higher than that of PY(pentenyl)TFSI. This unique results of PY(butyl)TFSI result from weaker interactions between the butyl group and Li^+ ions. The potential windows of the ILs depend mainly on the oxidation power of the functional group of PY^+ ions and were stable above 5.0 V, which is a sufficient potential range as the electrolyte for Li ion batteries. The cathodic decomposition on the Pt electrode also showed very unique behaviors with their functional groups but all synthesized ILs showed evidence of forming a SEI layer on the graphite electrode. The peak currents at the reduction on the graphite electrode were 100 times stronger in PY(butyl)TFSI and PY(pentenyl)TFSI than in PY(butyronitrile)TFSI and PY(methyl butyrate)TFSI. Similar results were also observed on the LiCoO_2 electrode without any special decomposition peak. Therefore, it is clear that the difference of the currents results from the difference of the electrolyte conductivity, which is deeply related with the solvation strength between Li^+ ions and the functional groups of the ILs.

ACKNOWLEDGMENT

This research was supported by the Converging Research Center Program through the National Research Foundation of Korea (NRF) funded by the Ministry of Education, Science and Technology (2011K000646).

References

1. M. Galinski, A. Lewandowski, I. Stepniak, *Electrochimica Acta*, 51 (2006) 5567-5580.
2. H. Tokuda, K. Hayamizu, K. Ishii, M.A.B.H. Susan, M. Watanabe, *The Journal of Physical Chemistry B*, 108 (2004) 16593-16600.
3. V. Borgel, E. Markevich, D. Aurbach, G. Semrau, M. Schmidt, *Journal of Power Sources*, 189 (2009) 331-336.
4. S. Seki, Y. Ohno, H. Miyashiro, Y. Kobayashi, A. Usami, Y. Mita, N. Terada, K. Hayamizu, S. Tsuzuki, M. Watanabe, *Journal of the Electrochemical Society*, 155 (2008) A421.
5. K. Tsunashima, S. Kodama, M. Sugiya, Y. Kunugi, *Electrochimica Acta*, (2010).
6. Z. Fei, W.H. Ang, D. Zhao, R. Scopelliti, E.E. Zvereva, S.A. Katsyuba, P.J. Dyson, *The Journal of Physical Chemistry B*, 111 (2007) 10095-10108.
7. S. Fang, Y. Tang, X. Tai, L. Yang, K. Tachibana, K. Kamijima, *Journal of Power Sources*, (2010).

8. Z.B. Zhou, H. Matsumoto, K. Tatsumi, *Chemistry-A European Journal*, 12 (2006) 2196-2212.
9. A.Lewandowski, A. Swiderska-Mocek, *Journal of Power Sources*, 194 (2009) 601-609.
10. J.S. Lee, J.Y. Bae, H. Lee, N.D. Quan, H.S. Kim, H. Kim, *Journal of Industrial and Engineering Chemistry*, 10 (2004) 1086-1089.
11. J. Dupont, R.F. de Souza, P.A.Z. Suarez, *Chemical reviews*, 102 (2002) 3667-3692.
12. K. Suzuki, M. Yamaguchi, M. Kumagai, N. Tanabe, S. Yanagida, *Comptes Rendus Chimie*, 9 (2006) 611-616.
13. D. Zhao, Z. Fei, R. Scopelliti, P.J. Dyson, *Inorganic chemistry*, 43 (2004) 2197-2205.
14. L. Zhao, J. Yamaki, M. Egashira, *Journal of Power Sources*, 174 (2007) 352-358.
15. W.L.F. Armarego, C.L.L. Chai, Purification of laboratory chemicals, *Butterworth Heinemann*, 2009.
16. K. Goossens, K. Lava, P. Nockemann, K. Van Hecke, L. Van Meervelt, K. Driesen, C. Gorller Walrand, K. Binnemans, T. Cardinaels, *Chemistry-A European Journal*, 15 (2009) 656-674.
17. P. Nockemann, M. Pellens, K. Van Hecke, L. Van Meervelt, J. Wouters, B. Thijs, E. Vanecht, T.N. Parac Vogt, H. Mehdi, S. Schaltin, *Chemistry-A European Journal*, 16 (2010) 1849-1858.
18. J.E. Gordon, G.N.S. Rao, *Journal of the American Chemical Society*, 100 (1978) 7445-7454.
19. S. Fang, L. Yang, J. Wang, M. Li, K. Tachibana, K. Kamijima, *Electrochimica Acta*, 54 (2009) 4269-4273.
20. S. Fang, L. Yang, C. Wei, C. Jiang, K. Tachibana, K. Kamijima, *Electrochimica Acta*, 54 (2009) 1752-1756.
21. K. Tsunashima, M. Sugiya, *Electrochemistry Communications*, 9 (2007) 2353-2358.
22. J. Lee, N. Quan, J. Hwang, J. Bae, H. Kim, B. Cho, H. Kim, H. Lee, *Electrochemistry Communications*, 8 (2006) 460-464.
23. H.B. Han, K. Liu, S.W. Feng, S.S. Zhou, W.F. Feng, J. Nie, H. Li, X.J. Huang, H. Matsumoto, M. Armand, *Electrochimica Acta*, (2010).
24. G.B. Appetecchi, M. Montanino, D. Zane, M. Carewska, F. Alessandrini, S. Passerini, *Electrochimica Acta*, 54 (2009) 1325-1332.
25. K. Hayamizu, Y. Aihara, *Electrochimica Acta*, 49 (2004) 3397-3402.
26. S. Randstrom, M. Montanino, G.B. Appetecchi, C. Lagergren, A. Moreno, S. Passerini, *Electrochimica Acta*, 53 (2008) 6397-6401.
27. V. Koch, L. Dominey, C. Nanjundiah, M. Ondrechen, *Journal of the Electrochemical Society*, 143 (1996) 798.
28. N.S. Choi, S.W. Ryu, J.K. Park, *Electrochimica Acta*, 53 (2008) 6575-6579